First Observation of the Four-Proton Unbound Nucleus ^{18}Mg

Y. Jin,[1, *] C. Y. Niu,[2, *] K. W. Brown,[2, 3, †] Z. H. Li,[1, ‡] H. Hua,[1, §]

A. K. Anthony,[2, 4] J. Barney,[2, 4] R. J. Charity,[5] J. Crosby,[2, 4] D. Dell'Aquila,[2] J. M. Elson,[5] J. Estee,[2, 4] M. Ghazali,[2, 4]

G. Jhang,[2] J. G. Li,[1, 6, 7] W. G. Lynch,[2, 4] N. Michel,[6, 7] L. G. Sobotka,[5, 8] S. Sweany,[2, 4] F. C. E. Teh,[2, 4]

A. Thomas,[5] C. Y. Tsang,[2, 4] M. B. Tsang,[2, 4] S. M. Wang,[9, 10] H. Y. Wu,[1] C. X. Yuan,[11] and K. Zhu[2, 4]

[1] *School of Physics and State Key Laboratory of Nuclear Physics and Technology, Peking University, Beijing 100871, China*
[2] *National Superconducting Cyclotron Laboratory, Michigan State University, East Lansing, Michigan 48824, USA*
[3] *Department of Chemistry, Michigan State University, East Lansing, Michigan 48824, USA*
[4] *Department of Physics and Astronomy, Michigan State University, East Lansing, Michigan 48824, USA*
[5] *Department of Chemistry, Washington University, St. Louis, Missouri 63130, USA*
[6] *Institute of Modern Physics, Chinese Academy of Sciences, Lanzhou 730000, China*
[7] *School of Nuclear Science and Technology, University of Chinese Academy of Sciences, Beijing 100049, China*
[8] *Department of Physics, Washington University, St. Louis, Missouri 63130, USA*
[9] *Institute of Modern Physics, Fudan University, Shanghai 200433, China*
[10] *FRIB Laboratory, Michigan State University, East Lansing, Michigan 48824, USA*
[11] *Sino-French Institute of Nuclear Engineering and Technology, Sun Yat-Sen University, Zhuhai 519082, China*
(Dated: December 30, 2021)

^{18}Mg was observed, for the first time, by the invariant-mass reconstruction of ^{14}O + $4p$ events. The ground-state decay energy and width are $E_T = 4.865(34)$ MeV and $\Gamma = 115(100)$ keV, respectively. The observed momentum correlations between the five particles are consistent with two sequential steps of prompt $2p$ decay passing through the ground state of ^{16}Ne. The invariant-mass spectrum also provides evidence for an excited state at an excitation energy of 1.84(14) MeV, which is likely the first excited 2^+ state. As this energy exceeds that for the 2^+ state in ^{20}Mg, this observation provides an argument for the demise of the $N = 8$ shell closure in nuclei far from stability. However, in open systems this classical argument for shell strength is compromised by Thomas-Ehrman shifts.

Introduction.—Wrinkled along the proton drip line are $1p$ and $3p$ emitters, for odd-Z isotopes, and $2p$ emitters for even-Z isotopes. The existence of the latter exotic decay, i.e., two-proton radioactivity, was predicted in the 1960s by Goldansky [1], and has been experimentally observed in many nuclei from ^{6}Be to ^{67}Kr [2–11]. By studying the momentum correlations in such three-body decays, one can access information about the structure of the nucleus prior to its decay [12].

For light nuclei, the relevant subsection of the chart of nuclei is displayed in Fig. 1. Several ground-state $2p$ emitters have been studied utilizing the invariant-mass method; these include ^{6}Be [2], ^{11,12}O [4, 5], ^{15,16}Ne [6, 7], and ^{19}Mg [8]. In this mass region, there are three nuclei known to undergo $3p$ emission, (^{7}B [13], ^{13}F [14], and ^{17}Na [15]). Prior to the work reported here, there has been only one observation of a $4p$ emitter, ^{8}C. The ground state of this exotic nucleus decays in two sequential steps of direct $2p$ emission, through the ground state of ^{6}Be [3]. In this Letter, we report the first observation of ^{18}Mg. The decay of its ground state is consistent with two sequential steps of direct $2p$ emission through the ground state of ^{16}Ne. We also report evidence for an excited state of ^{18}Mg. Most likely this state is the first 2^+ state and its relatively large excitation energy provides an argument for the demise of the $N = 8$ magic number at the proton drip line.

Experiment.—The experiment was performed at the National Superconducting Cyclotron Laboratory at Michigan State University. A primary beam of ^{24}Mg
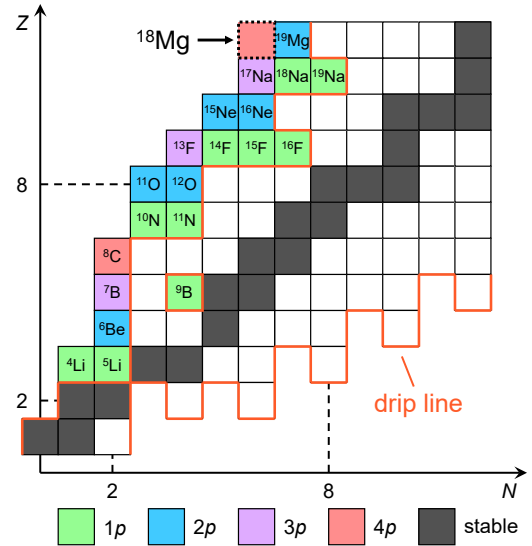

FIG. 1. Subsection of the chart of nuclei. Those nuclei which have been shown experimentally to decay by $1p$ (green), $2p$ (blue), $3p$ (purple), and $4p$ (pink) emissions are highlighted.

was accelerated through the Coupled Cyclotron Facility up to $E/A = 170$ MeV and fragmented on a ^{9}Be primary target. A secondary beam of ^{20}Mg at $E/A = 103$ MeV was then separated with the A1900 fragment separator [16, 17] with an intensity of 5600 pps and a purity of 31%. The incoming beam particles were identified on an

event-by-event basis via their time of flight between two plastic scintillators.

The ^{20}Mg beam impinged on a 1-mm-thick secondary ^{9}Be target, producing ^{18}Mg resonances via two-neutron knockout reactions, which promptly decay into ^{14}O and four protons. The protons were detected in an annular 1-mm-thick double-sided silicon-strip detector backed by an annular array of CsI(Tl) crystals, with polar angles subtending from $1.2°$ to $10.1°$ in the laboratory. The silicon detector is segmented into 128 pie-shaped sectors on one side and 128 concentric rings on the other [18]. The CsI(Tl) array was composed of twenty 50-mm-thick crystals, arranged in two concentric rings with 4 and 16 detectors in the inner and outer rings, respectively. Signals produced in the silicon strips were processed with the HINP16C analog chip electronics [19], while the signals of the CsI(Tl) array were processed by the conventional analog system. A 6-mm-thick aluminum absorber was placed in front of the silicon detector to protect it from scattered beam particles and to ensure the high-energy protons stop in the CsI(Tl) crystals.

The ^{14}O residues passed through the central hole of 10 mm diameter in the silicon detector and CsI(Tl) array, and were detected in an orthogonal array of scintillating fiber ribbons. Each ribbon was comprised of 64 square-cross-sectional fibers (0.25×0.25 mm^2). One end of each fiber was coupled to an 8×8 multianode photomultiplier and read out from its four edges with a resistive network. This scintillating-fiber array (SFA) provided the hit position of the ^{14}O residues close to the location of proton detection. The SFA improves the invariant-mass resolution by accurately measuring the relative angles between the exit-channel fragments thus eliminating the need to track the beam trajectory. The S800 spectrograph [20, 21] was used to provide the particle identification and energy of the residues.

The energy calibration of the silicon detector was made with a ^{232}U alpha source, while the CsI(Tl) detectors were calibrated using a 120 MeV proton beam and two degraders of different thicknesses. The calibration was verified by reconstructing the previously measured invariant mass of ^{16}Ne. From the present data, we obtain $Q_{2p}(^{16}\mathrm{Ne_{g.s.}}) = 1.425(4)$ MeV, a value consistent with the AME2020 atomic mass evaluation value of 1.401(20) MeV [22]. The quoted errors for decay energies of ^{16}Ne and ^{18}Mg extracted in this work are statistical. Based on comparison to known resonances, we assign an additional systematic uncertainty of 30 keV on the centroids.

Experimental results.—The spectrum of the total decay energy E_T constructed from the invariant mass of all detected ^{14}O + $4p$ events is shown in Fig. 2. Two peaks can be clearly resolved above a smooth background. The background has been modeled with a third-order polynomial, and likely arises from nonresonant continuum decay or high-lying wide resonances. The decay energy of the ground state was found to be $Q_{4p} = 4.865(34)$ MeV.
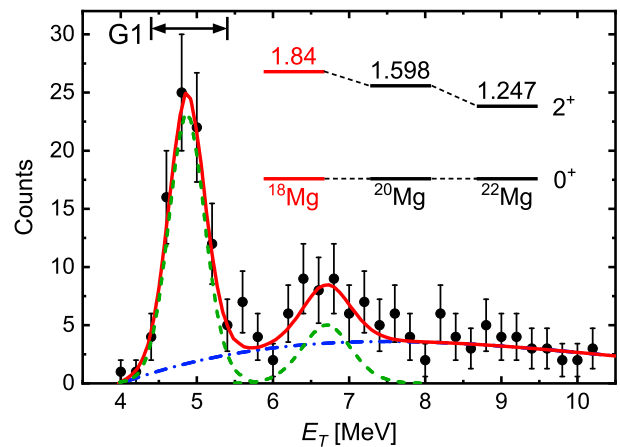

FIG. 2. Decay energy (E_T) spectrum for all detected ^{14}O + $4p$ events. The solid-red curve shows the fitted spectrum with the contributions for each state given by the dashed-green curves and the smooth background by the dashed-dotted-blue curve. The short solid vertical lines indicate the gate (G1) used to select ^{18}Mg$_{\mathrm{g.s.}}$ events. The inset shows the excitation energies of the first 2^+ states of the light magnesium isotopes. The numbers give the excitation energies in MeV of the 2^+ states.

While this is lower than the earlier values of 5.271(100) and 5.634(34) MeV predicted by a potential model [23] and the improved Kelson-Garvey mass relations [24], respectively, it comes within the uncertainty of the predicted value of 5.241(360) MeV by a parametrization method based on mirror energy differences [25]. In addition, a very recent calculation by Gamow shell model gives a prediction of 4.898 MeV [26], which is very close to the experimental result and will be discussed in detail below.

The second resonance is at $E_T = 6.71(14)$ MeV, which corresponds to an excitation energy of 1.84(14) MeV. This resonance is likely the first 2^+ state, which would then have an upward shift of around 250 keV from the known value of 1.588(8) MeV in the mirror ^{18}C [27]. The inset to Fig. 2 shows the excitation energies of the first 2^+ states, $E(2_1^+)$, for the three even-even, proton-rich magnesium isotopes. The $E(2_1^+)$ values increase from ^{22}Mg ($N = 10$) to ^{18}Mg ($N = 6$), i.e. across $N = 8$, possibly indicating the loss of this shell gap in magnesium.

The widths of the peaks in the invariant-mass spectrum shown in Fig. 2 are a folding of the intrinsic decay widths of the resonances and the experimental resolution. To extract the intrinsic decay widths, Monte Carlo simulations were performed assuming Breit-Wigner intrinsic line shapes for the resonances, with the experimental resolution and E_T-dependent efficiency incorporated. An energy resolution scaling factor for the CsI(Tl) detectors was included and fine tuned to reproduce the $2p$ invariant mass of the narrow ground state of ^{19}Mg [8, 28]. With the best fit of the CsI(Tl) resolution and its uncertainty, the intrinsic widths of the ground state and 2^+ state in
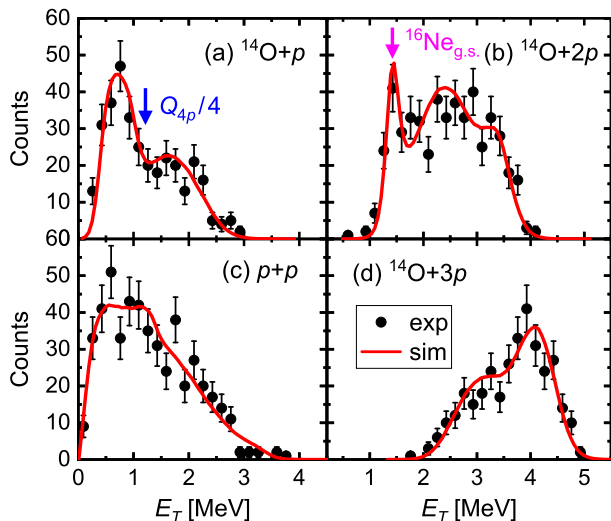
FIG. 3. Decay energy (E_T) spectra for the indicated subsystems of $^{18}\text{Mg}_{\text{g.s.}}$. Due to the combinatorial options, each event contributes four, six, six, and four entries to the spectra in panels (a), (b), (c), and (d), respectively. Red lines are the results of simulations assuming $^{18}\text{Mg}_{\text{g.s.}}$ decays to $^{14}\text{O} + 4p$ by two sequential steps of direct two-proton decay through $^{16}\text{Ne}_{\text{g.s.}}$, where the decay correlations are assumed to be the same as those observed for $^{16}\text{Ne}_{\text{g.s.}}$. The arrow in (a) is located at a quarter of the total ground-state decay energy where the corresponding distribution should peak for prompt $4p$ decay. The arrow in (b) shows the decay energy of the ground state of ^{16}Ne.

^{18}Mg have been determined to be 115(100) and 266(150) keV, respectively. The experimental resolutions at the centroids of the two peaks are 520 and 640 keV, respectively.

The decay of $^{18}\text{Mg}_{\text{g.s.}}$ is studied by examination of the decay-energy spectra of the four subsystems ($^{14}\text{O}+p$, $^{14}\text{O}+2p$, $^{14}\text{O}+3p$, $p+p$), see Fig. 3. The events were selected using the gate G1 shown in Fig. 2, where the fitted background under the peak is only 11% and can be largely ignored. Taking the second of these subsystems as an example, the relative energy of each of the six possible $^{14}\text{O}+2p$ subsystems is calculated and used to increment the spectrum shown in Fig. 3(b). If $^{18}\text{Mg}_{\text{g.s.}}$ decays through $^{16}\text{Ne}_{\text{g.s.}}$, then one of the six combinations will give us the real (and known) decay energy for $^{16}\text{Ne}_{\text{g.s.}}$ decaying to $^{14}\text{O} + 2p$ while the other five (wrong) combinations will contribute to a background in the relative energy spectrum. The background should be largely at higher energy as these combinations select protons from the first $^{18}\text{Mg}_{\text{g.s.}}$ decay step that has more decay energy (3.44 MeV) as compared to the second (1.42 MeV). This is in fact observed, i.e. a peak at around 1.4 MeV [see arrow in Fig. 3(b)] with a background of far larger integrated intensity at higher energy. The other three types of subevents also contain information on the correlations contained in the five-body exit channel.

In order to use all of the information in the four subevent spectra, we have constructed a Monte Carlo simulation of $^{18}\text{Mg}_{\text{g.s.}}$ decay, with subevent selection, where the experimental resolution and efficiency have been considered. These simulations are fitted simultaneously to all four subevent types shown in Fig. 3 with only one fitting parameter—a common scaling. The red curves in Fig. 3 are the simulated results for $^{18}\text{Mg}_{\text{g.s.}}$ decay assuming two sequential steps of direct two-proton decay, that is, $^{18}\text{Mg}_{\text{g.s.}} \rightarrow ^{16}\text{Ne}_{\text{g.s.}} + 2p$, followed by $^{16}\text{Ne}_{\text{g.s.}} \rightarrow ^{14}\text{O}_{\text{g.s.}} + 2p$. The two decay steps were both sampled from the known $^{16}\text{Ne}_{\text{g.s.}}$ decay correlations [7], that are dominated by the emission of two $s_{1/2}$ protons [29]. This simulation reproduces all subevent distributions indicating that the decay of $^{18}\text{Mg}_{\text{g.s.}}$ is consistent with two sequential steps of direct $2p$ emission. This agreement also suggests a large $s_{1/2}$ occupancy in $^{18}\text{Mg}_{\text{g.s.}}$ as is the case in $^{16}\text{Ne}_{\text{g.s.}}$.

While a realistic simulation of prompt five-body decay is beyond our present abilities, there is one aspect of such a decay that can be considered. In prompt $2p$ decay, the two core+p relative energies are approximately the same [2, 7, 10, 29] as this maximizes the product of their barrier penetration factors. Similarly in $4p$ decay, we expect the four core+p relative energies to be approximately the same. Thus for $4p$ decay, the $^{14}\text{O}+p$ distribution in Fig. 3(a) should peak at a quarter of the ground-state decay energy which is indicated by the arrow. Clearly we can rule out prompt $4p$ decay as the dominant decay mechanism, but a minor contribution is possible.

An alternative way to create a $^{16}\text{Ne}_{\text{g.s.}}$ intermediate state is via two initial steps of sequential one-proton decay. If such a decay passed through one narrow ^{17}Na intermediate, then we would have expected to see an unexplained peak in Fig. 3(d) associated with its decay. On the other hand, if a very-wide ^{17}Na intermediate state is involved, then this is basically the same as a prompt $2p$ decay to ^{16}Ne. However, we cannot rule out the possibility of decays through multiple ^{17}Na intermediate states which may give rise to similar correlations. Presently only one ^{17}Na state has been identified with a decay energy $Q_{3p} = 4.85(6)$ MeV [15], which is close to the limit of what is energetically allowed for $Q_{4p} = 4.865(34)$ MeV.

Theory.—As the newly discovered nuclide is a resonance, a continuum cognizant structure model is required. We choose to compare to the Gamow shell model (GSM) [30] as this model has very recently been used to make predictions for ^{18}Mg [26] and has also been used to calculate the excitation energies of the first 2^+ states for $A \approx 20$ nuclei [31]. In the GSM, the employed Berggren basis contains bound, resonance and scattering one-body states. This allows the incorporation of continuum coupling and generation of many-body nuclear wave functions with asymptotic forms appropriate for halo or resonance states. By comparison, the standard
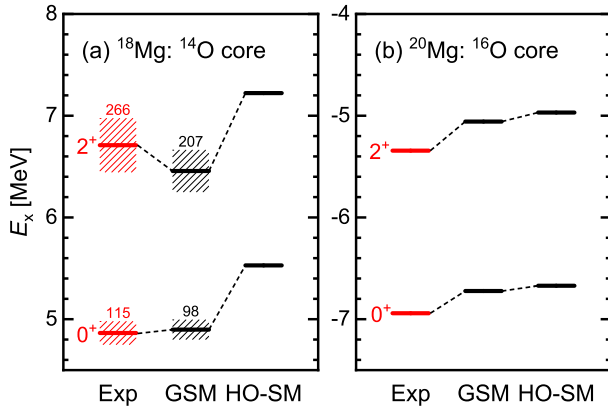
FIG. 4. Comparison of experimental results and the theoretical calculations of GSM and HO-SM. The energy levels in (a) ^{18}Mg and (b) ^{20}Mg are relative to the ^{14}O $+$ $4p$ and ^{16}O $+$ $4p$ thresholds, respectively. The shaded bars and the numbers above (units keV) indicate the decay widths of the ^{18}Mg states observed in this work and from the predictions of Gamow shell model.

TABLE I. GSM and HO-SM results for the ESPEs of the proton $1s_{1/2}$ and $0d_{5/2}$ orbits in ^{18}Mg and ^{20}Mg, as well as the proton occupation numbers (n_p) of these orbits for the 0_1^+ and 2_1^+ states. ESPEs are in MeV.

		GSM			HO-SM		
		ESPE	$n_p(0_1^+)$	$n_p(2_1^+)$	ESPE	$n_p(0_1^+)$	$n_p(2_1^+)$
^{18}Mg	$1s_{1/2}$	1.28	1.62	1.40	2.00	1.29	1.16
	$0d_{5/2}$	2.72	2.14	2.40	2.84	2.40	2.56
^{20}Mg	$1s_{1/2}$	0.76	0.27	0.45	1.12	0.22	0.36
	$0d_{5/2}$	-0.75	3.46	3.33	-0.74	3.32	3.22

harmonic-oscillator shell model (HO-SM) [32] is only formally suited for well-bound or well-quasi-bound nuclei [33].

To investigate the role that the continuum coupling plays in the structures of ^{18}Mg resonances and bound ^{20}Mg states, the HO-SM calculations using the same interaction as GSM [26, 31] have also been made. For ^{20}Mg [Fig. 4 (b)], the levels given by GSM and HO-SM are close in energy with no significant differences. However, for ^{18}Mg [Fig. 4(a)], these two models give energy levels differing by more than 600 keV. The actual decay energy of the ground state of ^{18}Mg is nicely reproduced by the GSM but not by the HO-SM. The GSM marginally over-suppresses the energy of the 2^+ state in ^{18}Mg, relative to the HO-SM, but comes closer to the actual value than the latter. The GSM also produces widths consistent with experiment as shown in Fig. 4(a).

The effective single-particle energies (ESPEs) and occupancies of the $1s_{1/2}$ and $0d_{5/2}$ proton orbits for ^{18}Mg and ^{20}Mg are given in Table I by the GSM and HO-SM. (The ESPEs are energies relative to the core.) As com-
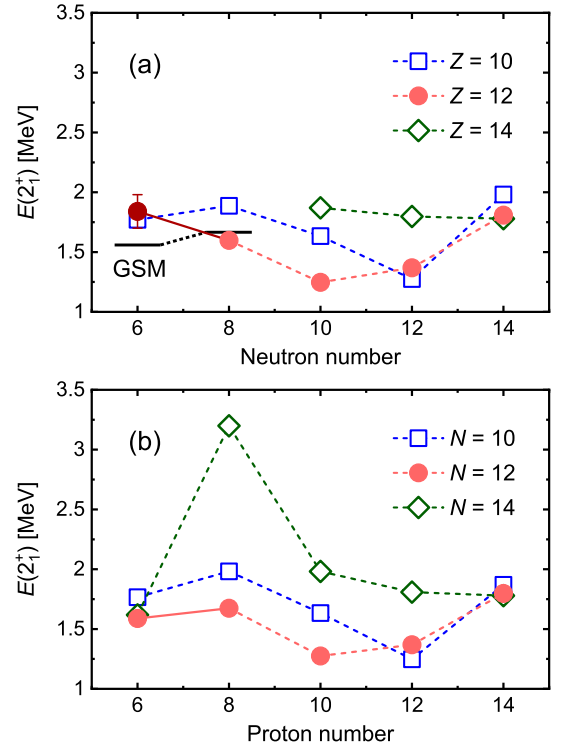

FIG. 5. Excitation energies of the first 2^+ states for a series of isotopes (a) and isotones (b) for Z or $N = 10$, 12, and 14. The dark red point in (a) shows the first experimental value for ^{18}Mg (this work). For comparison, the results from the GSM for ^{18,20}Mg ($Z = 12$) are shown in panel (a) in black lines.

pared to the HO-SM, the effect of the continuum considered in the GSM is to lower the $1s_{1/2}$ energy in ^{18}Mg and increase its occupancy. While the same can be said for the more stable ^{20}Mg, the changes are much less. By comparison, the ESPEs of the $0d_{5/2}$ barely move. In both calculations the occupancy of $1s_{1/2}$ orbit is far greater in the lighter isotope and the coupling to the continuum increases the occupancy of this orbit for both the ground state and the 2^+ state.

2^+ *systematics.*— Figure 5 displays the evolution of the excitation energies for the first 2^+ states for isotopes (isotones) of $Z(N) = 10$, 12, and 14. For the isotonic systematics [Fig. 5 (b)], the maxima appear at $Z = 8$ for all three datasets. The $N = 14$ isotonic dataset displays the very large 2^+ excitation for ^{22}O, indicating the doubly magic nature of this nucleus [34, 35]. While the lightest silicon isotopes ($Z = 14$) are unknown, the existing isotopic data [Fig. 5(a)] are, with one exception, similar with the isotonic data, reflecting good mirror symmetry. For example the $N = 8$ maximum still remains in neon ($Z = 10$). The conspicuous exception is with the new datum for ^{18}Mg. The 2^+ excitation energy of ^{18}Mg ($N = 6$) is slightly higher than that of ^{20}Mg ($N = 8$), the opposite of what would be expected if $N = 8$ were

magic at $Z = 12$, and opposite to the trend for the mirrors. This aspect of the 2^+ evolution is not predicted by the GSM [see Fig 5(a)]. Taken at face value, this larger 2^+ excitation energy and the large quadrupole deformation of ^{20}Mg (extracted from inelastic deuteron scattering [36]) support the argument that $N = 8$ shell gap is weakened at the proton drip line. However, it is also true that the 2^+ excitation energy is impacted by differential Thomas-Ehrman shifts [37, 38]. While the GSM predicts similar downshifts for the two levels [Fig. 4(a)], if the 2^+ downshift was reduced due to a smaller $s_{1/2}$ occupancy compared to its value in Table I, the predicted excitation energy would be increased. Further studies are needed to disentangle these two effects.

Conclusions.—We have observed, for the first time, ^{18}Mg via its decay into $4p + ^{14}$O. The ground-state decay energy was found to be $E_T = 4.865(34)$ MeV. The decay of the ground state of this nucleus is consistent with two sequential steps of $2p$ decay. Another state at 1.84(14) MeV of excitation was also observed and it is likely the first 2^+ state. Comparing this excitation energy to that for the first excited state of ^{20}Mg possibly indicates a weakening of the $N = 8$ shell closure in magnesium. The Gamow shell model and harmonic-oscillator shell model were used to study the effects of coupling to the continuum. The former, but not the latter, can reproduce the ground-state properties. However, the Gamow shell model does not predict that the 2_1^+ excitation energy is higher in ^{18}Mg than in ^{20}Mg. Extending the studies to $N = 8$ at $Z = 14$, i.e., ^{22}Si, would help with the interpretation of these trends.

---

* Y. Jin and C. Y. Niu contributed equally to this work.

† brownk@nscl.msu.edu

‡ zhli@pku.edu.cn

§ hhua@pku.edu.cn

[1] V. I. Goldansky, On neutron-deficient isotopes of light nuclei and the phenomena of proton and two-proton radioactivity, Nucl. Phys. **19**, 482 (1960).

[2] I. A. Egorova, R. J. Charity, L. V. Grigorenko, Z. Chajecki, D. Coupland, J. M. Elson, T. K. Ghosh, M. E. Howard, H. Iwasaki, M. Kilburn, *et al.*, Democratic Decay of ^{6}Be Exposed by Correlations, Phys. Rev. Lett. **109**, 202502 (2012).

[3] R. J. Charity, J. M. Elson, J. Manfredi, R. Shane, L. G. Sobotka, Z. Chajecki, D. Coupland, H. Iwasaki, M. Kilburn, J. Lee, *et al.*, 2p-2p decay of ^{8}C and isospin-allowed 2p decay of the isobaric-analog state in ^{8}B, Phys. Rev. C **82**, 041304(R) (2010).

[4] T. B. Webb, S. M. Wang, K. W. Brown, R. J. Charity, J. M. Elson, J. Barney, G. Cerizza, Z. Chajecki, J. Estee, D. E. M. Hoff, *et al.*, First Observation of Unbound ^{11}O, the Mirror of the Halo Nucleus ^{11}Li, Phys. Rev. Lett. **122**, 122501 (2019).

[5] R. A. Kryger, A. Azhari, M. Hellström, J. H. Kelley, T. Kubo, R. Pfaff, E. Ramakrishnan, B. M. Sherrill, M. Thoennessen, S. Yokoyama, *et al.*, Two-Proton Emission from the Ground State of ^{12}O, Phys. Rev. Lett. **74**, 860 (1995).

[6] F. Wamers, J. Marganiec, F. Aksouh, Yu. Aksyutina, H. Álvarez-Pol, T. Aumann, S. Beceiro-Novo, K. Boretzky, M. J. G. Borge, M. Chartier, *et al.*, First Observation of the Unbound Nucleus ^{15}Ne, Phys. Rev. Lett. **112**, 132502 (2014).

[7] K. W. Brown, R. J. Charity, L. G. Sobotka, Z. Chajecki, L. V. Grigorenko, I. A. Egorova, Yu. L. Parfenova, M. V. Zhukov, S. Bedoor, W. W. Buhro, *et al.*, Observation of Long-Range Three-Body Coulomb Effects in the Decay of ^{16}Ne, Phys. Rev. Lett. **113**, 232501 (2014).

[8] I. Mukha, K. Sümmerer, L. Acosta, M. A. G. Alvarez, E. Casarejos, A. Chatillon, D. Cortina-Gil, J. Espino, A. Fomichev, J. E. García-Ramos, *et al.*, Observation of Two-Proton Radioactivity of ^{19}Mg by Tracking the Decay Products, Phys. Rev. Lett. **99**, 182501 (2007).

[9] B. Blank, A. Bey, G. Canchel, C. Dossat, A. Fleury, J. Giovinazzo, I. Matea, N. Adimi, F. De Oliveira, I. Stefan, *et al.*, First observation of ^{54}Zn and its decay by two-proton emission, Phys. Rev. Lett. **94**, 232501 (2005).

[10] K. Miernik, W. Dominik, Z. Janas, M. Pfützner, L. Grigorenko, C. R. Bingham, H. Czyrkowski, M. Ćwiok, I. G. Darby, R. Dabrowski, *et al.*, Two-Proton Correlations in the Decay of ^{45}Fe, Phys. Rev. Lett. **99**, 192501 (2007).

[11] T. Goigoux, P. Ascher, B. Blank, M. Gerbaux, J. Giovinazzo, S. Grévy, T. Kurtukian Nieto, C. Magron, P. Doornenbal, G. G. Kiss, *et al.*, Two-Proton Radioactivity of ^{67}Kr, Phys. Rev. Lett. **117**, 162501 (2016).

[12] M. Pfützner, M. Karny, L. V. Grigorenko, and K. Riisager, Radioactive decays at limits of nuclear stability, Rev. Mod. Phys. **84**, 567 (2012).

[13] R. J. Charity, J. M. Elson, J. Manfredi, R. Shane, L. G. Sobotka, B. A. Brown, Z. Chajecki, D. Coupland, H. Iwasaki, M. Kilburn, *et al.*, Investigations of three-, four-, and five-particle decay channels of levels in light nuclei created using a ^{9}C beam, Phys. Rev. C **84**, 014320 (2011).

[14] R. J. Charity, T. B. Webb, J. M. Elson, D. E. M. Hoff, C. D. Pruitt, L. G. Sobotka, K. W. Brown, G. Cerizza, J. Estee, W. G. Lynch, *et al.*, Observation of the Exotic Isotope ^{13}F Located Four Neutrons beyond the Proton Drip Line, Phys. Rev. Lett. **126**, 132501 (2021).

[15] K. W. Brown, R. J. Charity, J. M. Elson, W. Reviol, L. G. Sobotka, W. W. Buhro, Z. Chajecki, W. G. Lynch, J. Manfredi, R. Shane, *et al.*, Proton-decaying states in light nuclei and the first observation of ^{17}Na, Phys. Rev. C **95**, 044326 (2017).

[16] D. J. Morrissey, B. M. Sherrill, M. Steiner, A. Stolz,

and I. Wiedenhoever, Commissioning the A1900 projectile fragment separator, Nucl. Instrum. Methods Phys. Res., Sect. B **204**, 90 (2003).

[17] A. Stolz, T. Baumann, T. N. Ginter, D. J. Morrissey, M. Portillo, B. M. Sherrill, M. Steiner, and J. W. Stetson, Production of rare isotope beams with the NSCL fragment separator, Nucl. Instrum. Methods Phys. Res., Sect. B **241**, 858 (2005).

[18] S4 Design by Micron Semiconductor Ltd., http://www.micronsemiconductor.co.uk/product/s4/.

[19] G. L. Engel, M. Sadasivam, M. Nethi, J. M. Elson, L. G. Sobotka, and R. J. Charity, A multi-channel integrated circuit for use in low- and intermediate-energy nuclear physics—HINP16C, Nucl. Instrum. Methods Phys. Res., Sect. A **573**, 418 (2007).

[20] D. Bazin, J. A. Caggiano, B. M. Sherrill, J. Yurkon, and A. Zeller, The S800 spectrograph, Nucl. Instrum. Methods Phys. Res., Sect. B **204**, 629 (2003).

[21] J. Yurkon, D. Bazin, W. Benenson, D. J. Morrissey, B. M. Sherrill, D. Swan, and R. Swanson, Focal plane detector for the S800 high-resolution spectrometer, Nucl. Instrum. Methods Phys. Res., Sect. A **422**, 291 (1999).

[22] M. Wang, W. J. Huang, F. G. Kondev, G. Audi, and S. Naimi, The AME 2020 atomic mass evaluation (II). Tables, graphs and references, Chin. Phys. C **45**, 030003 (2021).

[23] H. T. Fortune and R. Sherr, Mass of ^{18}Mg(g.s.), Phys. Rev. C **87**, 044315 (2013).

[24] J. Tian, N. Wang, C. Li, and J. Li, Improved Kelson-Garvey mass relations for proton-rich nuclei, Phys. Rev. C **87**, 014313 (2013).

[25] H. T. Fortune, Masses of ^{17,18,19,20}Mg, Phys. Rev. C **94**, 044305 (2016).

[26] N. Michel, J. G. Li, F. R. Xu, and W. Zuo, Proton decays in ^{16}Ne and ^{18}Mg and isospin-symmetry breaking in carbon isotopes and isotones, Phys. Rev. C **103**, 044319 (2021).

[27] Evaluated Nuclear Structure Data File (ENSDF), https://www.nndc.bnl.gov/ensdf/.

[28] P. Voss, T. Baumann, D. Bazin, A. Dewald, H. Iwasaki, D. Miller, A. Ratkiewicz, A. Spyrou, K. Starosta, M. Thoennessen, C. Vaman, and J. A. Tostevin, ^{19}Mg two-proton decay lifetime, Phys. Rev. C **90**, 014301 (2014).

[29] T. B. Webb, R. J. Charity, J. M. Elson, D. E. M. Hoff, C. D. Pruitt, L. G. Sobotka, K. W. Brown, J. Barney, G. Cerizza, J. Estee, *et al.*, Particle decays of levels in ^{11,12}N and ^{12}O investigated with the invariant-mass method, Phys. Rev. C **100**, 024306 (2019).

[30] N. Michel, W. Nazarewicz, M. Płoszajczak, and T. Vertse, Shell model in the complex energy plane, J. Phys. G **36**, 013101 (2008).

[31] N. Michel, J. G. Li, F. R. Xu, and W. Zuo, Description of proton-rich nuclei in the $A \approx 20$ region within the Gamow shell model, Phys. Rev. C **100**, 064303 (2019).

[32] E. Caurier, G. Martínez-Pinedo, F. Nowacki, A. Poves, and A. P. Zuker, The shell model as a unified view of nuclear structure, Rev. Mod. Phys. **77**, 427 (2005).

[33] J. Dobaczewski, N. Michel, W. Nazarewicz, M. Płoszajczak, and J. Rotureau, Shell structure of exotic nuclei, Prog. Part. Nucl. Phys. **59**, 432 (2007).

[34] P. G. Thirolf, B. V. Pritychenko, B. A. Brown, P. D. Cottle, M. Chromik, T. Glasmacher, G. Hackman, R. W. Ibbotson, K. W. Kemper, T. Otsuka, L. A. Riley, and H. Scheit, Spectroscopy of the 2_1^+ state in ^{22}O and shell structure near the neutron drip line, Phys. Lett. B **485**, 16 (2000).

[35] E. Becheva, Y. Blumenfeld, E. Khan, D. Beaumel, J. M. Daugas, F. Delaunay, Ch-E. Demonchy, A. Drouart, M. Fallot, A. Gillibert, *et al.*, $N = 14$ Shell Closure in ^{22}O Viewed through a Neutron Sensitive Probe, Phys. Rev. Lett. **96**, 012501 (2006).

[36] J. S. Randhawa, R. Kanungo, M. Holl, J. D. Holt, P. Navrátil, S. R. Stroberg, G. Hagen, G. R. Jansen, M. Alcorta, C. Andreoiu, *et al.*, Observation of excited states in ^{20}Mg sheds light on nuclear forces and shell evolution, Phys. Rev. C **99**, 021301(R) (2019).

[37] J. B. Ehrman, On the displacement of corresponding energy levels of C^{13} and N^{13}, Phys. Rev. **81**, 412 (1951).

[38] R. G. Thomas, An analysis of the energy levels of the mirror nuclei, C^{13} and N^{13}, Phys. Rev. **88**, 1109 (1952).